Interplay between nonclassicality and $\mathcal{PT}$ symmetry in an effective two-level system with open system effects

Javid Naikoo,[1,*] Subhashish Banerjee,[1,†] and Anirban Pathak[2,‡]
[1]*Indian Institute of Technology Jodhpur, Jodhpur 342011, India*
[2]*Jaypee Institute of Information Technology, A-10, Sector-62, Noida UP-201309, India*

(Received 3 May 2019; published 22 August 2019)

A three-level atom in Λ configuration is reduced to an effective two-level system, under appropriate conditions, and its $\mathcal{PT}$ symmetric properties are investigated. This effective qubit system, when subjected to a beam-splitter type of interaction, provides the scope of directly (indirectly) probing the nonclassical properties of the output (input) state. Here, we study nonclassical properties of the output state by using some well-known measures of nonclassical correlations like the measurement-induced disturbance, concurrence, and negativity. The nonclassical features are found to enhance in the $\mathcal{PT}$ symmetric (PTS) phase compared to the $\mathcal{PT}$ symmetry broken (PTB) phase. Further, the output ports of the beam splitter are subjected to different quantum noise channels, both non-Markovian, e.g., random telegraph noise as well as Markovian, e.g., phase damping and amplitude damping noise. The application of noise channels is found to decrease the degree of nonclassicality, though continuing to exhibit distinct behavior in PTS and PTB phases, with the dominant behavior appearing in the former case. Further, the results are compared with the case when dynamics is governed by a Hermitian Hamiltonian. This allows one to demarcate the contributions to nonclassicality from different types of dynamics.

DOI: 10.1103/PhysRevA.100.023836

I. INTRODUCTION

In textbook quantum mechanics, one of the fundamental axioms is that the physical observables are represented by the Hermitian operators which always possess real eigenvalues and conserve the probability [1]. In particular, the Hamiltonian H generating the time evolution of the system has real eigenvalues and the corresponding time translation operator $U = e^{-iHt}$ is unitary as a consequence of Hermiticity of H. However, a non-Hermitian Hamiltonian with the parity ($\mathcal{P}$) - time ($\mathcal{T}$) symmetry, often referred to as a $\mathcal{PT}$ symmetric Hamiltonian, can also possess a real eigenvalue spectrum [2]. Such non-Hermitian Hamiltonians may undergo a spontaneous transition to the $\mathcal{PT}$ symmetry broken phase [3]. The operators $\mathcal{P}$ and $\mathcal{T}$ are defined by their action on the dynamical variables $\hat{x}$ (the position operator) and $\hat{p}$ (the momentum operator), such that the *linear* operator $\mathcal{P}$ acts as $\hat{p} \to -\hat{p}$ and $\hat{x} \to -\hat{x}$, while the *antilinear* operator $\mathcal{T}$ acts such that $\hat{p} \to -\hat{p}, \hat{x} \to \hat{x}$. Further, $\mathcal{T}$ also flips the sign of $i = \sqrt{-1}$, i.e., it transforms $i \to -i$, such that the commutation relation $[\hat{x}, \hat{p}] = i$ is preserved. The $\mathcal{PT}$ symmetric systems can exhibit *exceptional points* (EPs) where the eigenvalues of the non-Hermitian Hamiltonian are degenerate. At these points, the Hamiltonian is not diagonalizable and the geometric eigenvectors of the Hamiltonian no longer span the underlying Hilbert space, rather the complete Hilbert space is spanned by the geometric eigenvectors supplemented by so-called algebraic eigenvectors of the same (nondiagonalizable) Hamiltonian (see [4,5] and the references therein).

The $\mathcal{PT}$ symmetric Hamiltonians belong to a more general class of pseudo-Hermitian systems [6]. The eigenfunctions of a system Hamiltonian in the $\mathcal{PT}$ symmetric phase are also the eigenfunctions of the $\mathcal{PT}$ operator, i.e., all eigenfunctions are also $\mathcal{PT}$ symmetric. However, in the PTB phase, some or all the eigenvalues become complex and not all the eigenfunctions of the Hamiltonian possess $\mathcal{PT}$ symmetry. With these interesting properties, the non-Hermitian quantum mechanics has attracted a lot of attention, leading to the exploration of $\mathcal{PT}$ symmetric systems in different domains. The *phase lapses* observed in the experiments with Aharonov-Bohm rings remained a puzzle until the phenomenon was explained using the non-Hermitian Hamiltonian [7,8]. The non-Hermitian Hamiltonians have been used to describe the laser-induced continuum structures in atoms [9,10]. In [11], a scheme based on *resonance coalescence* to achieve vibrational cooling was proposed. The extension of $\mathcal{PT}$ symmetric quantum mechanics to quantum field theory with cubic interaction was reported in [12]. Further, the role of non-Hermicity in open quantum systems has been explored in [13,14]. The dominance of the Lyapunov exponent over the non-Hermicity parameters leads to real eigenvalues in the Hatano-Nelson non-Hermitian Anderson model for disordered systems [15]. Based on Lagrangian principles a formalism was developed to describe coupled optical $\mathcal{PT}$ symmetric systems [16]. In [17], it was demonstrated that the $\mathcal{PT}$ symmetric potentials can exhibit phenomena such as double refraction, power oscillations, and secondary emissions. The existence of solitons in optical $\mathcal{PT}$ symmetric systems was reported in [18]. These solitons were found to be stable over a wide range of potential parameters. The concept of *pseudo-$\mathcal{PT}$*

*naikoo.1@iitj.ac.in
†subhashish@iitj.ac.in
‡anirban.pathak@jiit.ac.in

symmetry was introduced in [19], where it was shown that one can manipulate $\mathcal{PT}$ symmetry properties in periodically modulated optical systems with balanced gain and loss. The quantum phase transition and its connection with the geometric phase was studied in the non-Hermitian $\mathcal{PT}$ symmetric Ising model [5,20]. A non-Hermitian, $\mathcal{PT}$ symmetric model of the dimerized spin chain was introduced in [21] and its (anti-)ferromagnetic quantum phase transition was analyzed. The $\mathcal{PT}$ symmetric systems with spontaneous generation of photons and superradiant emission of radiation were also investigated in [22,23].

From a practical point of view, $\mathcal{PT}$ symmetry has found many important applications such as the single-mode $\mathcal{PT}$ lasers [24,25], unidirectional reflectionless $\mathcal{PT}$ symmetric metamaterial at optical frequencies [26]. Based on $\mathcal{PT}$ symmetry, many new photonic devices have been designed and fabricated [27,28]. The $\mathcal{PT}$ symmetric periodic structures act as unidirectional electromagnetically induced transparency (EIT) devices near the exceptional point [29]. A $\mathcal{PT}$ symmetric coupler under appropriate conditions can act as an optical switch [30]. Further, $\mathcal{PT}$ symmetry has made the notion of *loss* useful, which was otherwise considered as a detrimental physical effect [31].

The above mentioned features and applications of $\mathcal{PT}$ symmetry and the potential application of entanglement in quantum computing and communication have motivated us to look for a $\mathcal{PT}$ symmetric physical system which can be realized experimentally and which can generate entanglement. In what follows, such a system will be studied.

Effective Hamiltonians in quasiopen systems related to microwave cavities have been investigated in [32] with regard to $\mathcal{PT}$ symmetric subconfigurations and effective $\mathcal{PT}$ phase transitions. It is worth mentioning here that the non-Hermitian Hamiltonian, in the context of open quantum systems [33], are often referred to as *effective* Hamiltonians H_{eff}, governing the dynamics in a restrictive subspace of the quantum system and appear as von Neumann–type evolution in the master equations [13,34–36]. Thus, the notion of $\mathcal{PT}$ symmetry has proved to be a useful tool in probing the behavior of dynamics of the systems described by effective Hamiltonians which correspond to non-Hermititan systems. Since the degree of quantumness of a system is controlled by the underlying dynamics, this naturally invites one to explore the interplay between nonclassicality and $\mathcal{PT}$ symmetry in such systems [37–43].

In this work, we will analyze the behavior of nonclassical correlations, quantified by well-known measures of quantum correlations viz., measurement-induced disturbance (MID) [44], concurrence [45–47], and negativity in a $\mathcal{PT}$ symmetric system. This will be achieved by using a Λ-type atom, i.e., a three-level atom in which a state is coupled by radiative interaction to two other states lying below it (energetically) which have no radiative coupling between them. This three-level system is reduced to an effective two-level system with the underlying Hamiltonian bearing $\mathcal{PT}$ symmetry. The resulting qubit is combined with vacuum at the beam splitter (or through an interaction which is mathematically equivalent to a beam-splitter operation), and the output state is analyzed for the above mentioned nonclassicality measures [48,49].

The paper is organized as follows: In Sec. II, we discuss beam-splitter operation and how it can be used to probe the nonclassicality of a single qubit state. This is followed by a discussion of various measures of nonclassicality. Section III is devoted to detailed discussion of the model consisting of a $\mathcal{PT}$ symmetric system. In Sec. IV, we analyze the effect of various quantum noise channels on the nonclassical feature of the output state. Results and their discussion are presented in Sec. V. We conclude in Sec. VI.

II. NONCLASSICALITY FOR A SINGLE INPUT STATE AT BEAM SPLITTER

A single qubit state when fed to one port of a beam splitter and the vacuum at the other port, results in a bipartite state which may exhibit nonclassical properties including entanglement [48,50]. Specifically, at the output of the beam splitter a two-mode entangled state is obtained if and only if the state (other than the vacuum state) fed into the input is a single-mode nonclassical state. Thus, the nonclassicality of the single-mode input state gets transferred to a two-mode entangled state, and one can try to measure the nonclassicality of the input state by measuring the entanglement of the output state [48,50]. For a particular beam-splitter setting, the behavior of the nonclassical properties of the output state is entirely controlled by the input state parameters. Since we are not considering optical qubits, in the present study, a beam-splitter operation is visualized as an operation described by an interaction Hamiltonian which is mathematically equivalent to the beam-splitter Hamiltonian.

A. Beam-splitter input-output state

In what follows, we plan to analyze the nonclassicality of the simplest quantum state, a qubit state, parametrized by $p \in [0, 1]$, and x such that $|x| \in [0, \sqrt{p(1-p)}]$ and given by

$$\rho(p;x) \equiv [\rho_{mn}] = \begin{pmatrix} 1-p & x \\ x^* & p \end{pmatrix}. \tag{1}$$

Such states, when combined with the vacuum at a beam splitter, result in the output state being separable (if the input qubit state is classical) or entangled (if the input qubit state is nonclassical). This statement is not restricted to the usual optical beam splitter. In fact, there are many physical systems whose Hamiltonians (thus, the operation and the physical consequence of the operation) are equivalent to that of the usual beam splitter. For example, we can think of the easy to visualize systems like a symmetric linear optical coupler [51] or double-well atom-atom Bose Einstein condensates (BECs), where each well contains a BEC, but particle exchange is allowed in such a way that the total number of particles is conserved [52]. Such setups described by effective $\mathcal{PT}$-symmetric Hamiltonians have also been studied in [53] and discussed in [54]. The Hamiltonian of these systems are equivalent to that of the usual beam splitter. Now, extending this discussion to the context of the present work, we may note that the atomic beam splitter was realized long ago [55] where atoms were diffracted from cleaved ionic crystals. As a result, the electronic states of an atom were found to be slightly shifted when approaching the atomic surface. More

recently, an atomic beam splitter (more precisely dark state beam splitter) has been realized for metastable helium having two dark states which are relatively stable [56]. A magneto-optical beam splitter for atoms was reported in [57]. Many of the initially designed or proposed atomic beam splitters were based on tunneling, and were not robust. A robust beam splitter on an atomic chip was introduced for the guided atoms in [58]. Another class of atomic beam splitters involves the interaction of an atom with electric or magnetic dipole moment with static electric or magnetic fields. A detailed account of the beam-splitter operations with the atom can be found in [59]. In short, there are various physical systems (especially atomic systems) which are operationally equivalent to the conventional beam splitter, and in all those cases the resulting output state can be used to directly probe the nonclassicality (entanglement) of the output state and thus indirectly probe the nonclassical properties of the input state. Here the output state can be expressed as

$$\rho_{\text{out}}(\theta) = \mathrm{U_{BS}}(\rho \otimes |0\rangle\langle 0|)\mathrm{U_{BS}}^{\dagger}, \tag{2}$$

where $\mathrm{U_{BS}} = \exp(-\frac{i}{\hbar}H\theta)$ corresponds to a unitary transformation of the beam-splitter operation. The balanced beam-splitter operation is characterized by $\theta = \pi/2$[1] and can be generated by the Hamiltonian $H = \frac{i\hbar}{2}(a_1^{\dagger}a_2 - a_1 a_2^{\dagger})$, with $a_1(a_2)$ being the annihilation operators for the two input modes. Physical realization of this Hamiltonian is easy for optical qubits. However, for the atomic system, this can be realized by using pulses of appropriate shape and frequency. Specifically, we may note that the balanced beam-splitter operation $\mathrm{U_{BS}}$ performed on the product input-state $\rho \bigotimes |0\rangle\langle 0|$ can be decomposed in terms of standard quantum gates as $\mathrm{U_{BS}} = (\mathrm{CS})(\mathrm{T}\bigotimes\mathrm{T})\sqrt{\mathrm{SWAP}}$, where CS corresponds to a controlled S gate, and T and $\sqrt{\mathrm{SWAP}}$ are different quantum logic gates whose details can be found in [61,62]. As all these gates can be realized for atomic qubits, an operation equivalent to $\mathrm{U_{BS}}$ can also be realized for the atomic system of our interest. In the rest of this work, we will deal with the balanced beam splitter and call $\rho_{\text{out}}(\theta = \pi/2)$ as ρ_{out}, given by

$$\rho_{\text{out}} = \begin{pmatrix} 1-p & \frac{ix}{\sqrt{2}} & \frac{x}{\sqrt{2}} & 0 \\ \frac{-ix^*}{\sqrt{2}} & \frac{p}{2} & \frac{-ip}{2} & 0 \\ \frac{x^*}{\sqrt{2}} & \frac{ip}{2} & \frac{p}{2} & 0 \\ 0 & 0 & 0 & 0 \end{pmatrix}. \tag{3}$$

The nonclassicality of this state can be probed using the well-known measures such as MID discerning the classical and quantum correlations exhibited by a system under the action of joint measurements on its subsystems and the entanglement measures such as concurrence and negativity, discussed next.

B. Measurement-induced disturbance

Consider a bipartite system described by the state ρ belonging to Hilbert space $\mathcal{H}_A \otimes \mathcal{H}_B$, where $\mathcal{H}_A$ and $\mathcal{H}_B$ represent the state space of systems A and B, respectively. One can construct the reduced state for one system by tracing over the other. Let ρ^A and ρ^B denote the reduced states for A and B; one can write

$$\rho^A = \sum_i p_i^A \Pi_i^A \quad \text{and} \quad \rho^B = \sum_j p_j^B \Pi_j^B. \tag{4}$$

Here, Π^A and Π^B are the projectors on the corresponding state space with eigenvalues p^A and p^B, respectively. One can define a joint measurement Π, in terms of the spectral resolution of reduced states, such that the postmeasurement state is given by

$$\Pi(\rho) = \sum_{i,j} \left(\Pi_i^A \otimes \Pi_j^B\right)\rho\left(\Pi_i^A \otimes \Pi_j^B\right). \tag{5}$$

If the postmeasurement state does not change under the action of Π, i.e., if $\Pi(\rho) = \rho$, we say that ρ is a classical state with respect to the measurement strategies $\{\Pi_i^A \otimes \Pi_j^B\}$; otherwise ρ is a legitimate quantum state. This idea was used to construct a measure of nonclassicality [44,63] given as follows:

$$Q(\rho) = I(\rho) - I(\Pi(\rho)). \tag{6}$$

Here, $I(\cdot)$ is the quantum mutual information defined as $I(\rho) = S(\rho^A) + S(\rho^B) - S(\rho)$ and $S(\cdot)$ is the von Neumann entropy. Note that for a classical state $I(\Pi(\rho)) = I(\rho)$, so $Q(\rho) = 0$. Therefore, Eq. (6) quantifies the difference between the quantum and classical correlations exhibited by a bipartite system.

C. Entanglement measures

In order to quantify the entanglement in a quantum system, several well-known measures have been proposed. These include entanglement of formation [64,65], entanglement of distillation [66], relative entropy of entanglement [67,68], and negativity [69,70]. For pure states, the Bell states provide an example of the maximally entangled states. However, in case of mixed states, defining a maximally entangled state is not straightforward. In this work, we use two entanglement measures, i.e., concurrence and negativity. The concurrence, as defined in [71], is given by

$$C(\rho) = \max[0, \lambda_1 - \lambda_2 - \lambda_3 - \lambda_4]. \tag{7}$$

Here, λ_i are eigenvalues of the matrix $\sqrt{\sqrt{\rho}\tilde{\rho}\sqrt{\rho}}$ and $\tilde{\rho} = (\sigma_y \otimes \sigma_y)\rho(\sigma_y \otimes \sigma_y)$ where σ_y is the Pauli matrix. Alternatively, λ_i represent the square roots of the eigenvalues of $\rho\tilde{\rho}$. The parameter C varies between 0 (unentangled states) to 1 (maximally entangled states). The negativity [69] is based on the positive partial transpose (PPT) criterion of separability and for a subsystem A is defined as

$$N(\rho) = \frac{||\rho^{\Gamma_A}||_1 - 1}{2}. \tag{8}$$

Here, ρ^{Γ_A} is the partial transpose of ρ with respect to the subsystem A. Equivalently, one can define the *negativity* as

$$N(\rho) = \sum_k \frac{|\lambda_k| - \lambda_k}{2}, \tag{9}$$

[1]The specific choice $\theta = \pi/2$ is made in consistency with the existing literature [60]. However, for other values of θ, the computation will become complex but the final conclusions of this paper would remain the same.

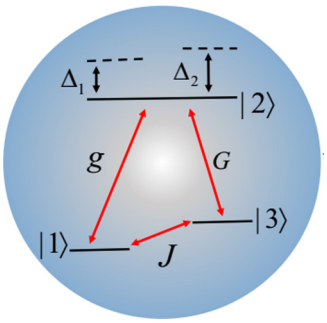

FIG. 1. Schematic illustration of three-level atom.

where $\{\lambda_k\}$ is the set of eigenvalues of the partial transposed matrix ρ^{Γ_A}. The nonclassical *potential* for the single-mode input state ρ is defined to be the amount of nonclassicality of the output state ρ_{out}. Consequently, the concurrence potential (CP) and negativity potential (NP)[2] are defined as [48]

$$\text{CP}(\rho) = C(\rho_{\text{out}}), \quad \text{NP}(\rho) = N(\rho_{\text{out}}). \tag{10}$$

Note that the nonclassical features of the output state are controlled by the input state parameters.

The above mentioned procedure is now applied to a specific system of an effective two-level atom interacting with a reservoir. This system exhibits $\mathcal{PT}$ symmetry in a certain parameter range, thereby allowing one to study the interplay between $\mathcal{PT}$ symmetry and nonclassicality.

III. MODEL

A three-level Λ-type atom, with decay modes associated with all the three levels, provides an example of a $\mathcal{PT}$ symmetric system [72,73]. In this work, we will deal with an effective two-level Hamiltonian, which is constructed by starting with a Λ-type system [74] shown in Fig. 1. The resulting qubit state with the general form given by Eq. (1), exhibits $\mathcal{PT}$ symmetry and can be fed to a beam splitter according to the local operation given in Eq. (2). This allows one to explore the nonclassicality of the output bipartite state, Eq. (3). This construction, therefore, provides a platform for studying the interplay between nonclassicality and $\mathcal{PT}$ symmetry of the above described system.

The Hamiltonian, in a rotating frame with respect to the optical modes, becomes

$$\begin{aligned} H = {} & \hbar\Delta_1 |1\rangle\langle 1| + \hbar\Delta_2 |3\rangle\langle 3| \\ & - \hbar[g|1\rangle\langle 2| + G|3\rangle\langle 2| + \Omega' e^{i\phi}|1\rangle\langle 3| + \text{H.c.}]. \end{aligned} \tag{11}$$

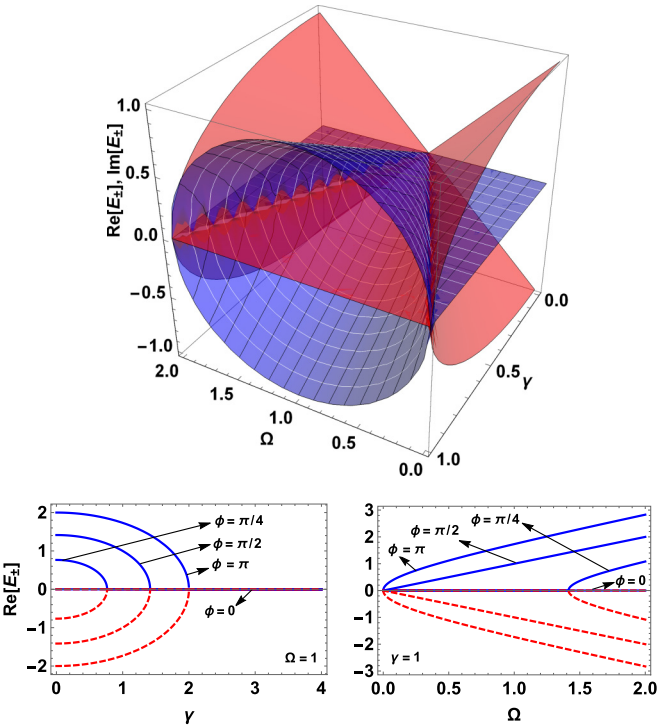

FIG. 2. Top plot depicts the real (lined-blue surface) and imaginary (plane-red surface) parts of the eigenvalues. Both real and imaginary eigenvalues occur in pairs symmetrically about $\text{Re}[E_\pm] = \text{Im}[E_\pm] = 0$. Bottom panel, presented here for clarity, depicts the real eigenvalues with respect to the parameters γ and Ω for different values of parameter ϕ.

Here, $\Delta_{1,2}$ are the detunings of the optical fields from the corresponding atomic resonances, and g and G are Rabi frequencies of the two optical fields. Ω' is the coupling strength due to the RF field, and the phase ϕ can be controlled via the adjustment of the relative phase between the RF field and the two optical fields.

For simplicity, we assume equal coupling strengths $g = G$ and same detuning $\Delta_1 = \Delta_2 = \Delta$, and use the notation $\frac{\Delta\Omega'}{G^2} = \Omega$. By assuming equal population gain and loss rates associated with levels 1 and 3, respectively, the following effective two-level Hamiltonian can be obtained [74]:

$$\begin{aligned} \mathcal{H}_{\text{eff}} = {} & (1 - \Omega e^{i\phi})|1\rangle\langle 3| + (1 - \Omega e^{-i\phi})|3\rangle\langle 1| \\ & + i\gamma|1\rangle\langle 1| - i\gamma|3\rangle\langle 3|. \end{aligned} \tag{12}$$

The eigenvalues of this Hamiltonian are

$$E_\pm = \pm\sqrt{J^2 - \gamma^2}, \tag{13}$$

with $J = |1 - \Omega e^{i\phi}|$. The eigenvalues are real, and hence the system is $\mathcal{PT}$ symmetric, when the effective coupling $1 - \Omega e^{i\phi}$ is greater than the gain and loss γ. The $\mathcal{PT}$ symmetry is said to be broken when the gain and loss exceeds the coupling strength. The borderline between the two regimes is such that the eigenvalues $E_\pm = 0$, called the exceptional points. The variation of energy with respect to the coupling Ω and gain and loss rate γ is shown in Fig. 2.

[2]In 2005, Asboth *et al.* [50] proposed that the measures of entanglement in the output mode of the beam splitter can be used to indirectly measure the nonclassicality of the input mode. Thus, in this approach, a conventional entanglement measure is not really used to measure entanglement, rather it is used to measure nonclassicality. To stress on this distinct feature, Asboth *et al.* referred to it as entanglement potential [50]. Subsequently it has become a convention and terms like concurrence potential are used frequently in analogy with the nomenclature used by Asboth [48].

Using the effective Hamiltonian of Eq. (12), one can therefore write the time-dependent Schrödinger equation as

$$i\frac{\partial\,|\Psi(t)\rangle}{\partial t} = \mathcal{H}_{\rm eff}\,|\Psi(t)\rangle\,, \tag{14}$$

such that the nonunitary time translation operator is given by

$$\mathcal{U}(t) = \begin{pmatrix} \cos(\omega t) + \frac{\gamma}{\omega}\sin(\omega t) & -i\frac{1-\Omega e^{i\phi}}{\omega}\sin(\omega t) \\ -i\frac{1-\Omega e^{-i\phi}}{\omega}\sin(\omega t) & \cos(\omega t) - \frac{\gamma}{\omega}\sin(\omega t) \end{pmatrix}. \tag{15}$$

Here, $\omega = \sqrt{J^2-\gamma^2}$. Let the initial state be $|\Psi(0)\rangle = |1\rangle \equiv (1\ \ 0)^T$ at time $t=0$. At a later time t, the normalized wave function becomes

$$|\Psi_{PT}(t)\rangle = \frac{\left[\cos(\omega t) + \frac{\gamma}{\omega}\sin(\omega t)\right]|1\rangle - i\frac{1-\Omega e^{-i\phi}}{\omega}\sin(\omega t)\,|3\rangle}{\langle\Psi_{PT}(t)|\Psi_{PT}(t)\rangle} \tag{16}$$

such that the probability of the atom being in states $|1\rangle$ and $|3\rangle$ is given by $|\langle 1|\Psi_{PT}(t)\rangle|^2$ and $|\langle 3|\Psi_{PT}(t)\rangle|^2$, respectively.

In the limit $\omega \to 0$, i.e., $J \to \gamma$, we approach the *exceptional points* where the normalized state vector is given by

$$|\Psi_{EP}(t)\rangle = \frac{(1+\gamma t)\,|1\rangle - i(1-\Omega e^{-i\phi})t\,|3\rangle}{\langle\Psi_{EP}(t)|\Psi_{EP}(t)\rangle}. \tag{17}$$

For comparison, we also consider the case when time evolution is generated by a Hermitian Hamiltonian such that the eigenvalues are numerically identical to those given by Eq. (13). As an example, we consider the Hermitian Hamiltonian,

$$H_H = \vec{r}\cdot\vec{\sigma}, \tag{18}$$

where $\vec{r} = (r_1, r_2, r_3)$ and $\vec{\sigma}$ denotes the Pauli triplet $(\sigma_1, \sigma_2, \sigma_3)$. The eigenvalues of H_H are $\pm|\vec{r}|$. Therefore, the condition $|\vec{r}| = J^2 - \gamma^2$, would allow one to demarcate the contributions to nonclassicality of the input state subjected to $\mathcal{PT}$ symmetric and Hermitian Hamiltonians. The unitary evolution is governed by the following operator:

$$\mathcal{U}_H(t) = \begin{pmatrix} \cos(rt) - \frac{ir_3}{r}\sin(rt) & \frac{-ir_1-r_2}{r}\sin(rt) \\ \frac{-ir_1+r_2}{r}\sin(rt) & \cos(rt) + \frac{ir_3}{r}\sin(rt) \end{pmatrix}. \tag{19}$$

Consequently, the state $|1\rangle = (1\,0)^T$ at time $t=0$ is time translated to the following normalized form at some later time t,

$$|\Psi_H(t)\rangle = \frac{\left(\cos(rt) - \frac{ir_3}{r}\sin(rt)\right)|1\rangle + \left(\frac{-ir_1-r_2}{r}\sin(rt)\right)|3\rangle}{\langle\Psi_H(t)|\Psi_H(t)\rangle}. \tag{20}$$

In what follows, we will use the states given in Eqs. (16), (17), and (20), as input to the beam splitter (along with the vacuum state) and analyze the resulting output state for different measures of nonclassicality viz., MID, concurrence, and negativity. In all our numerics, we will use the gain and loss parameter $\gamma = 0.5$ and $J = 0.6$ (for PTS phase) and $J = 0.4$ for PTB phase. Further, we choose $r_1 = 0$, $r_2 = 0.1$, and $r_3 \approx 0.317$. This choice (which is completely arbitrary) satisfies the condition $|\vec{r}| \approx J^2 - \gamma^2$ for the PTS phase and therefore allows us to compare the extent of nonclassicality in the PTS phase with that under Hermitian dynamics. Also, for the dynamics at *exceptional points* we will use $J = \gamma = 0.5$.

IV. EFFECT OF DIFFERENT QUANTUM NOISE CHANNELS ON NONCLASSICALITY

Evolution of quantum correlations in the presence of non-Markovian noise has been the subject matter of many studies [75–80]. However, to the best of our knowledge, the evolution of the dynamics of the quantum correlations present in a $\mathcal{PT}$ symmetric system has not been investigated earlier in the presence of noise.

In this section, we study the interplay between nonclassicality and $\mathcal{PT}$ symmetry when the output ports of the beam splitter are subjected to different *quantum noise channels*. Specifically, we consider random telegraph noise (RTN) [75,76,78,81], phase damping (PD) [82], and amplitude damping (AD) [83,84] channels. The RTN allows us to bring out the interplay between $\mathcal{PT}$ symmetry and non-Markovian dynamics. Non-Markovian evolution has been found to favor the suppression of decoherence and disentanglement [85,86]. Since one of the major challenges in carrying out quantum information tasks is to sustain the coherence and entanglement [87], non-Markovianity assisted control on the degree of coherence, and entanglement can become very pertinent in future.

Random telegraph noise. This model describes a qubit subjected to a classical source of random telegraph noise, i.e., a bistable fluctuator randomly switching between its two states with a given rate γ [88]. The ratio between the switching rate and the system-environment coupling, determines whether the system is Markovian or non-Markovian. The underlying time-dependent phenomenological Hamiltonian is $H_{\rm RTN} = \hbar\sum\Gamma_i(t)\sigma_i$, where σ_i are Pauli matrices and the independent random variables $\Gamma_i(t) = a_i n_i(t)$, with the random variable $n_i(t)$ having a Poisson distribution with mean $t/2\tau_i$ and a_i is a coin flip random variable assuming values $\pm a_i$. The bath correlation functions are given by $\langle\Gamma_j(t)\Gamma_k(t')\rangle = a_k^2\exp(-|t-t'|/\tau_k)\delta_{jk}$. In [89], it was shown that the complete positivity requires two of a_i be zero, which physically represents the situation of noise acting only in one direction. Assuming a_3 to be nonzero, the evolution is governed by the following Kraus operators,

$$K_0(t) = \sqrt{\frac{1+\Lambda(t)}{2}}\begin{pmatrix}1 & 0\\ 0 & 1\end{pmatrix},$$
$$K_1(t) = \sqrt{\frac{1-\Lambda(t)}{2}}\begin{pmatrix}1 & 0\\ 0 & -1\end{pmatrix}. \tag{21}$$

Here, the parameter $\Lambda(t) = \exp(-\gamma t)(\cos(\mu\gamma t) + \frac{\sin(\mu\gamma t)}{\mu})$ is called the *memory kernel* and is crucial for determining whether the dynamics is Markovian or non-Markovian. Also, $\mu = \sqrt{(\frac{2a}{\gamma})^2 - 1}$ and $\gamma = \frac{1}{2\tau}$. The parameter a is proportional to the strength of system-environment coupling. In the non-Markovian regime, the parameter μ is real and $\Lambda(t)$ an oscillatory function. In Markovian case, μ is purely imaginary leading to damped evolution. This demarcation can be

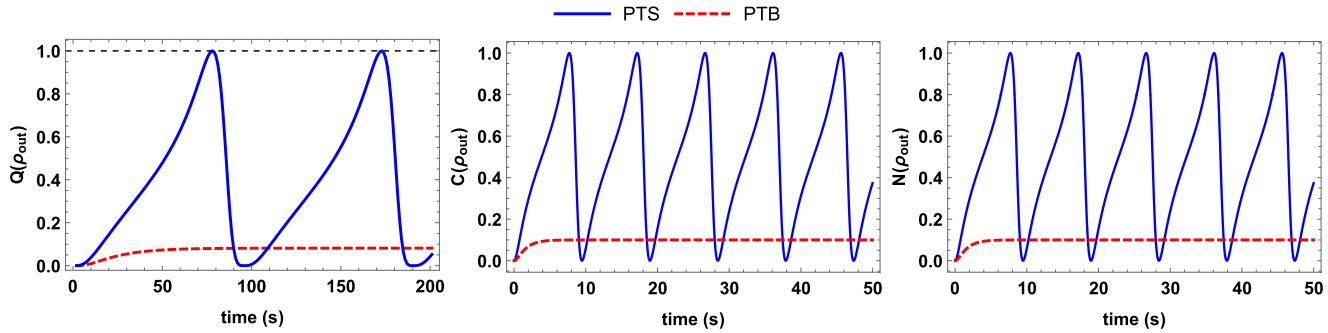

FIG. 3. MID $[Q(\rho_{\text{out}})]$, Concurrence $[C(\rho_{\text{out}})]$, and Negativity $[N(\rho_{\text{out}})]$ of the output state given in Eq. (3), with respect to time in seconds (s). The effective coupling between two levels is $J = |1 - \Omega e^{i\phi}|$ and the gain and loss rate is γ. The conditions $J > \gamma$ and $J < \gamma$ correspond to PTS and PTB regimes, respectively. The nonclassical features are enhanced in the PTS regime, that is, when system coupling dominates the gain and loss rate. This is in consonance with the results of our previous work [37].

controlled by the relative values of a and τ [78]. The Markovian and non-Markovian regimes are characterized by $4a\tau < 1$ and $4a\tau > 1$, respectively. For a general qubit at time $t = 0$, given by Eq. (1), the action of RTN map results in the state at time $t > 0$, give by

$$\rho(t) = \mathcal{E}^{\text{RTN}}_{t \leftarrow t_0}[\rho(0)] = \begin{pmatrix} 1-p & x\Lambda(t) \\ x^*\Lambda(t) & p \end{pmatrix}. \tag{22}$$

Phase damping. This noise process is uniquely quantum mechanical in nature and describes the loss of quantum information without loss of energy [82]. In this case, the Kraus operators are given by

$$K_0 = \begin{pmatrix} 1 & 0 \\ 0 & \sqrt{1-\lambda} \end{pmatrix} \quad \text{and} \quad K_1 = \begin{pmatrix} 0 & 0 \\ 0 & \sqrt{\lambda} \end{pmatrix}. \tag{23}$$

The parameter λ can be modeled as $1 - \cos^2(\eta t)$, with $0 \leqslant \eta t \leqslant \pi/2$. The action of PD channel on a general state [Eq. (1)] is as follows:

$$\mathcal{E}^{\text{PD}}_{t \leftarrow t_0}[\rho] = \begin{pmatrix} 1-p & x\sqrt{1-\lambda} \\ x^*\sqrt{1-\lambda} & p \end{pmatrix}. \tag{24}$$

Amplitude damping. This noise process is a schematic model for describing the energy dissipation effects due to loss of energy from a quantum system to its environment. The dynamics is given by the following Kraus operators [83]:

$$K_0 = \begin{pmatrix} 1 & 0 \\ 0 & \sqrt{1-\gamma} \end{pmatrix} \quad \text{and} \quad K_1 = \begin{pmatrix} 0 & \sqrt{\gamma} \\ 0 & 0 \end{pmatrix}. \tag{25}$$

The time-dependent parameter can be modeled by $\gamma = 1 - e^{-\chi t}$. Under the AD channel a general qubit state evolves as

$$\mathcal{E}^{\text{AD}}_{t \leftarrow t_0}[\rho] = \begin{pmatrix} 1-p(1-\gamma) & x\sqrt{1-\gamma} \\ x^*\sqrt{1-\gamma} & p(1-\gamma) \end{pmatrix}. \tag{26}$$

The implementation of the quantum noise channel at the output ports of the beam splitter can be realized by the combined action of such channels on a bipartite state $\rho(\alpha)$ [90]. Note that the channel acts on the output states of the form given by Eq. (3) and the input state is given by Eqs. (16), (17), and (20). We have

$$\rho(\alpha, q_1, q_2) = \sum_{i,j} [K_i(q_1) \otimes K_j(q_2)]\rho(\alpha)[K_i^\dagger(q_1) \otimes K_j^\dagger(q_2)]. \tag{27}$$

Here, q_1 and q_2 are the channel parameter and, in general, $q_1 \neq q_2$, Fig. 4. Using this description and the definition in Eq. (7), one obtains the following analytic expressions for concurrence,

$$C(\rho_{\text{out}}) = \begin{cases} p & \text{Noiseless} \\ p\Lambda_1\Lambda_2 & \text{RTN} \\ p\sqrt{(1-\lambda_1)(1-\lambda_2)} & \text{PD} \\ p\sqrt{(1-\gamma_1)(1-\gamma_2)} & \text{AD} \end{cases}. \tag{28}$$

Here, p is the probability as defined in Eq. (1). Unfortunately, the expressions for negativity turn out to be too complicated and are not given here. An interesting observation is that for $p = 0$ (and hence $x = 0$), that is, when both input ports of the beam splitter contain vacuum state, the concurrence of the output state becomes zero. The same is true for other nonclassical measures like MID and negativity. This is expected as the output state is expected to be nonclassical if one of the input states is vacuum and the other one is a nonclassical state, but the vacuum state is classical in the sense that it can be described by positive P function as it can be described as a coherent state having 0 photons. The nonclassical measure of the output state in all other cases reflects the degree of nonclassiclaity of the input state.

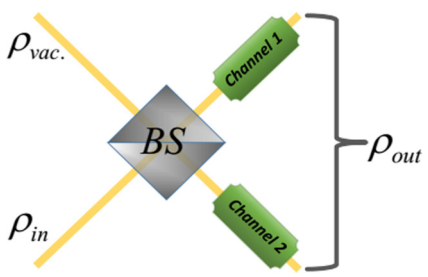

FIG. 4. Beam splitter (BS) with input states ρ_{in} and $\rho_{\text{vac}}(= |0\rangle\langle 0|)$. The output ports are subjected to a *channel*, leading to the final output state ρ_{out}. The channel parameters are, in general, different unless stated otherwise.

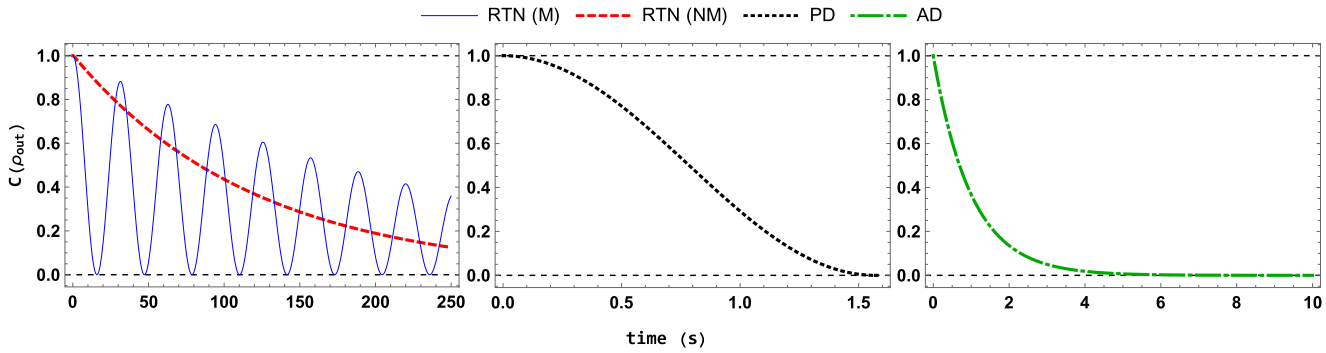

FIG. 5. Showing concurrence with respect to time when the state parameter $p = 1$ which corresponds to the input state $|1\rangle$ at the beam splitter. Left, middle, and right plots correspond to RTN, PD, and AD channels, respectively. The solid (blue) and dashed (red) curves in the left plot pertain to non-Markovian and Markovian processes, respectively. The channels at the two output ports are assumed to be identical, with the following parameters: for RTN, $a = 0.05$ and $\gamma = 0.002$ for the non-Markovian case, and $a = 0.05$ and $\gamma = 1.2$ for the Markovian case. Further, $\eta = 1$ and $\chi = 1$, for the PD and AD channels, respectively.

Another way of looking at the nonclassicality of the post channel output state, is by noting that a two-qubit state can be written, as discussed in the Appendix, in the following form:

$$|\psi_\alpha\rangle = \sqrt{\alpha}|01\rangle + \sqrt{1-\alpha}|10\rangle. \tag{29}$$

This state, when subjected to the PD channel, results in the following mixed state:

$$\rho_{\rm PD}(q,\lambda_1,\lambda_2) = \left(\tfrac{1}{2}-y\right)|\beta_1\rangle\langle\beta_1| + \left(\tfrac{1}{2}+y\right)|\beta_2\rangle\langle\beta_2| + \left(\alpha-\tfrac{1}{2}\right)(|\beta_1\rangle\langle\beta_2| + |\beta_2\rangle\langle\beta_1|),$$

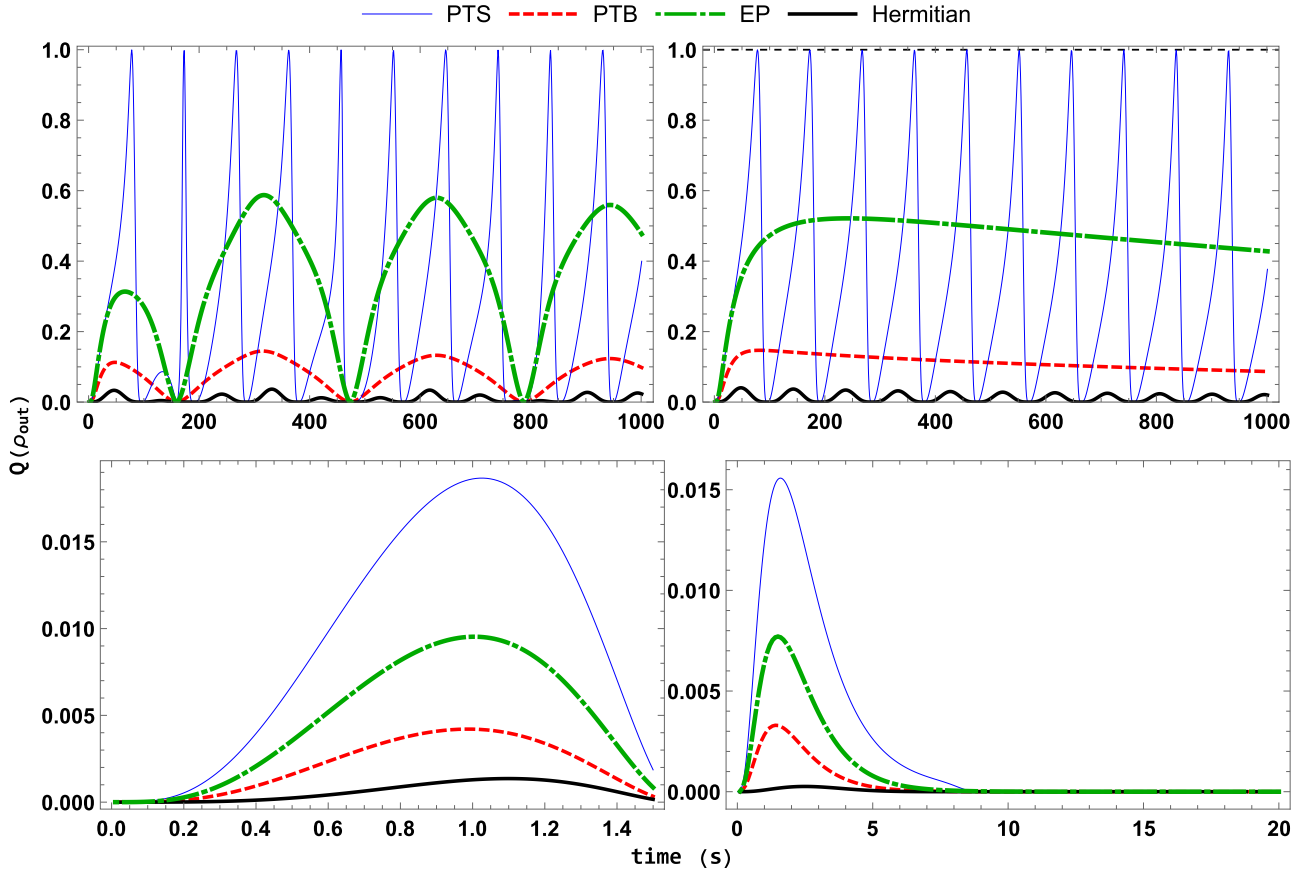

FIG. 6. MID $[Q(\rho_{\rm out})]$, as defined in Eq. (6), is plotted as a function of time when the output ports of the beam splitter are subjected to RTN noise in non-Markovian (top left) and Markovian (top right) regimes, respectively. The same quantity is shown for the PD channel (bottom left) and the AD channel (bottom right). Solid thin (blue) and dashed (red) curves correspond to the PTS and PTB phases, respectively, with the input state given in Eq. (16). Dot-dashed (green) curve depicts the behavior at exceptional points with the input state given in Eq. (17). Solid thick (black) curve corresponds to the case when the state evolves under the Hermitian Hamiltonian. The input state in this case is given in Eq. (20). The various channel parameters used are the same as in Fig. 5.

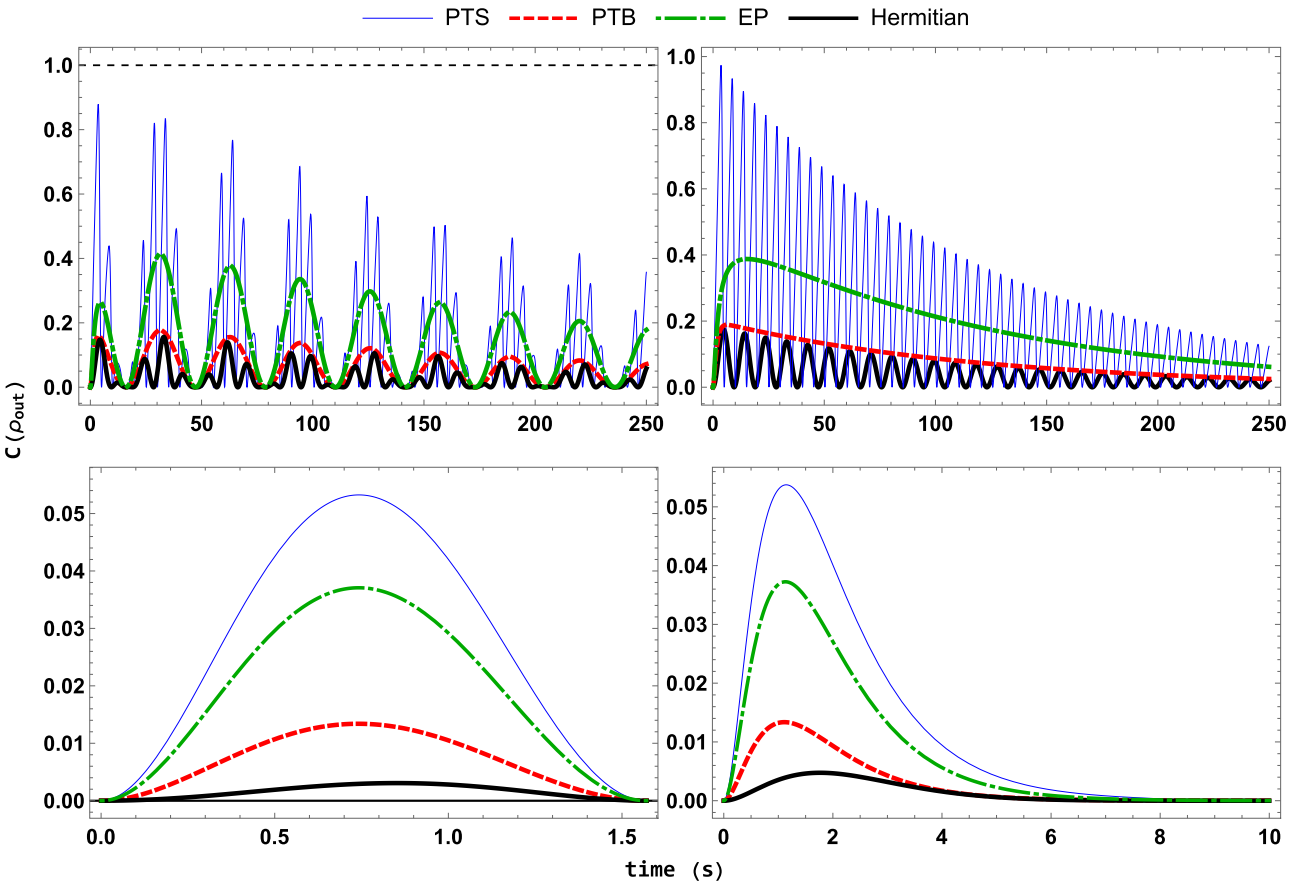

FIG. 7. Concurrence as a function of time when the output ports of the beam splitter are subjected to RTN noise in non-Markovian (top left) and Markovina (top right) regimes, respectively. The same quantity is shown for the PD channel (bottom left) and the AD channel (bottom right). The nomenclature for various curves is the same as in Fig. 6. The various channel parameters used are the same as in Fig. 5.

where $y = \sqrt{\alpha(1-\alpha)(1-\lambda_1)(1-\lambda_2)}$. If one sets $\alpha = \frac{1}{2}$ which means $p = 1$, then the above state becomes

$$\rho_{\rm PD}(q, \lambda_1, \lambda_2) = l_+|\beta_1\rangle\langle\beta_1| + l_-|\beta_2\rangle\langle\beta_2|.$$

Here, $l_\pm = (1 \pm \sqrt{(1-\lambda_1)(1-\lambda_2)})/2$. Thus, for the special case $p = 1$, we have the Bell-diagonal representation of the state Eq. (29). The concurrence for such states is given by

$$C = 2\max\left[0, \max_\pm[l_\pm] - \tfrac{1}{2}\right] = \sqrt{(1-\lambda_1)(1-\lambda_2)}. \quad (30)$$

This is consistent with Eq. (28) for $p = 1$.

V. RESULTS AND DISCUSSION

The output state of the beam splitter when the output ports are not subjected to noise channel is given in Eq. (3) which is in terms of the input state parameters p and x. We consider the case when the input state is given by Eq. (16). This allows us to study the interplay between nonclassiclaity of the state and the $\mathcal{PT}$ symmetry of the underlying system (Fig. 1). The real eigenvalues, Fig. 2, imply complete $\mathcal{PT}$ symmetry(also called the exact $\mathcal{PT}$ symmetry) [6] of the underlying effective Hamiltonian, Eq. (12).

In order to investigate the nonclassicality of the output state, we study the well-known measures such as MID, concurrence, and negativity. These quantities are depicted in Fig. 3 with respect to time. Enhancement in the magnitude of these measures is observed in the PTS phase compared to the PTB phase. This enhancement in nonclassicality can be attributed to the fact that in the PTS phase, the coupling strengths dominate the loss and gain rate.

Things become interesting when the output ports of the beam splitter are subjected to the noisy quantum channels, as illustrated in Fig. 4. In this work, we considered three important channels, viz., RTN, PD, and AD. These channels provide distinct dynamical features with RTN allowing both Markovian as well as non-Markovian behavior, while PD and AD admit Markovian dynamics. The channels on the output ports could be the same or different depending on the channel parameters. Here, we have considered the same channels on both output ports. In Fig. 5, the concurrence of the output state, when the input state is $(0\,1)^T$, is depicted with respect to time. In particular, under the RTN evolution, the dynamics in non-Markovian and Markovian regimes is contrasted by the characteristic recurrent behavior in the former case. The concurrence evolves under the RTN channel as follows:

$$C(\rho_{\rm out})|_{p=1} = e^{(-\tilde{\gamma}_1 t)}\left[\cos(\mu_1\tilde{\gamma}_1 t) + \frac{\sin(\mu_1\tilde{\gamma}_1 t)}{\mu_1}\right] \times e^{(-\tilde{\gamma}_2 t)}\left[\cos(\mu_2\tilde{\gamma}_2 t) + \frac{\sin(\mu_2\tilde{\gamma}_2 t)}{\mu_2}\right]. \quad (31)$$

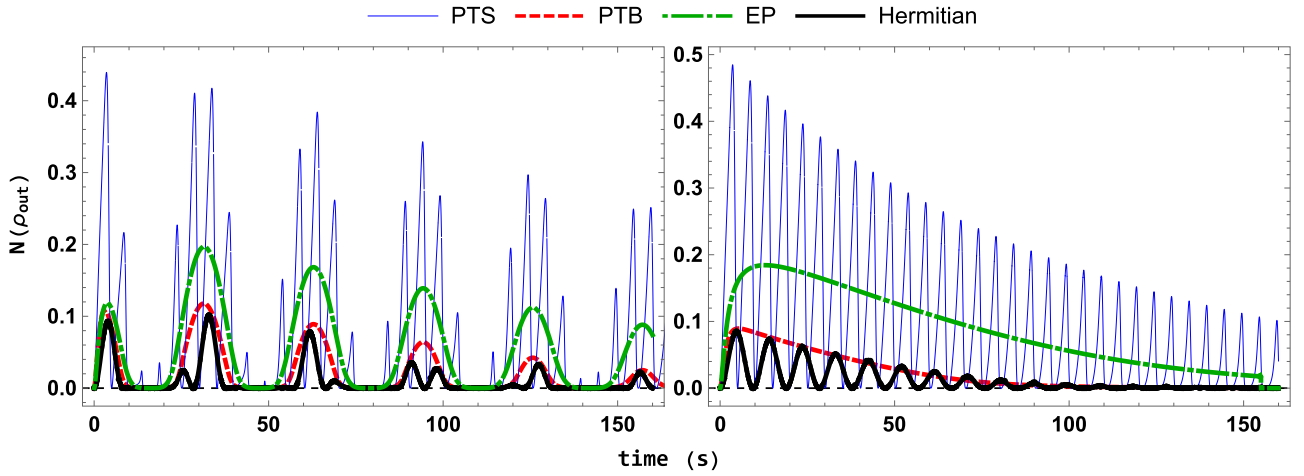

FIG. 8. Negativity as a function of time when the output ports of the beam splitter are subjected to RTN noise in non-Markovian (left) and Markovian (right) regimes, respectively. The nomenclature for various curves is the same as in Fig. 6. The various channel parameters used are the same as in Fig. 5.

The evolution is non-Markovian or Markovian according to μ_i $(i = 1, 2)$ being real or imaginary. We have considered the case in which the channels on the output ports are identical, that is, $\tilde{\gamma}_1 = \tilde{\gamma}_2$ and $\mu_1 = \mu_2$. In non-Markovian regime, one observes an enhancement in the concurrence and thus the entanglement, as compared with the Markovian case. In contrast, the behavior of concurrence in PD and AD channels shows the typical decrease with time.

We now analyze the behavior of various measures of nonclassicality when the input state is evolving under the $\mathcal{PT}$ symmetric Hamiltonian and is given by Eq. (16). The output state is subjected to various noise models. The results are compared with the case when the input state is time evolved by a Hermitian Hamiltonian with the corresponding unitary operator given in Eq. (19). Figure 6 shows the measurement-induced disturbance (MID) quantified by the parameter $\mathcal{Q}(\rho_{\text{out}})$. Although, the application of the noise channels results in decreasing the degree of nonclassicality (quantified by the maximum value) of various measures, nevertheless, the nonclassicality measures continue to show distinct behavior in PTS and PTB regimes, with enhanced magnitude in the former case. The curve depicting the behavior at exceptional points lies between the two regimes. In the Hermitian regime, the nonclassical features are found to be least in magnitude, for the particular values of parameters chosen. Further, in case of RTN noise, the non-Markovian regime is seen to show the typical recurrent behavior. Similar behavior is observed in the cases of concurrence (Fig. 7) and negativity (Fig. 8). The oscillating feature of the measures of nonclassiclaity in the Markovian regime of RTN as well as in case of PD and AD channels should not be confused with the characteristic recurrent behavior of non-Markovian dynamics. This feature appears due to the oscillatory nature for the input state given in Eq. (16), and can be seen from Fig. 5, where the input state is $|1\rangle = (0\ \ 1)^T$, T being the transpose operation.

VI. CONCLUSION

We considered a Λ-type three-level atom and derived an effective two-level system with $\mathcal{PT}$ symmetry. The $\mathcal{PT}$ symmetry is governed by the coupling strength between the two levels and their respective loss and gain rate, such that when the coupling dominated the loss and gain rate, the system is in the $\mathcal{PT}$ symmetric phase. However, when the gain and loss dominates the coupling, the system is said to be in the $\mathcal{PT}$ broken phase. Consequently, the eigenvalues of the underlying effective Hamiltonian are real and imaginary in the former and latter cases, respectively.

The beam splitter provides an elegant way of analyzing the nonclassical properties of the output state when the qubit at the input is combined with vacuum. We investigated various measures of nonclassicality, viz., measurement-induced disturbance (MID), concurrence, and negativity of the output state when the input state is the effective qubit state of our $\mathcal{PT}$ symmetric system. The nonclassical measures behave quite different in PTS and PTB regimes, depicting an enhancement of nonclassicality in the former case. Further, the application of various noise channels is accompanied with a decrease in the degree of nonclassicality. However, the nonclassicality measures continue to show distinct behavior in PTS and PTB phases, dominating in the former case. We considered three noise channels viz., non-Markovian random telegraph noise (RTN) as well as Markovian phase damping (PD), and amplitude damping (AD) channels and analyzed the behavior of various nonclassical measures under the influence of these channels. The results of the $\mathcal{PT}$ symmetric system are compared with the case when the time evolution is generated by a Hermitian Hamiltonian. This allows one to demarcate the contributions to nonclassicality from the two types of dynamics. For the specific values of parameters used, it is found that $\mathcal{PT}$ symmetric dynamics shows enhanced nonclassical features compared to the Hermitian counterpart. This study, therefore brings an interesting interplay of the quantumness of a system, along with its memory, and its $\mathcal{PT}$ symmetry, a property which is controlled by the coupling strength and the loss and gain rate associated with the energy levels of the system. The conceptual ideas and methods introduced here are quite general, and the same can be used to study the dynamics of various other physical systems. For example, a comparative study of all types of three-level

systems [72,73] in the context $\mathcal{PT}$ symmetry is ongoing currently.

APPENDIX

In order to analyze the effect of various quantum channels on the nonclassical properties of the output state ρ_{out} subjected to quantum noise channels, we rewrite the general bipartite state in a useful form. Consider a general two-party system with the underlying Hilbert spaces denoted by $\mathcal{H}_1$ and $\mathcal{H}_2$ with the corresponding bases $\{|0\rangle_1, |1\rangle_1\}$ and $\{|0\rangle_2, |1\rangle_2\}$, respectively. The tensor product state can be defined as

$$|w\rangle = \beta_{00}|0\rangle_1 \otimes |0\rangle_2 + \beta_{01}|0\rangle_1 \otimes |1\rangle_2 + \beta_{10}|1\rangle_1 \otimes |0\rangle_2 + \beta_{11}|1\rangle_1 \otimes |1\rangle_2 . \tag{A1}$$

This can also be viewed as a matrix,

$$M_w = (\beta_{ij}) = \begin{pmatrix} a & b \\ c & d \end{pmatrix}. \tag{A2}$$

According to the *singular value decomposition* theorem, any matrix can be written as a product $UDV^\dagger$, where both U and V are orthogonal matrices and D is a diagonal matrix. The elements of D are called *singular values*. Therefore, we have

$$M_w = UDV^\dagger. \tag{A3}$$

In order to diagonalize M_w, we note that the columns of both U and V matrices form orthogonal basis, therefore,

$$U = (|u_0\rangle \quad |u_1\rangle) \qquad \text{and} \quad V^\dagger = \begin{pmatrix} \langle v_0| \\ \langle v_1| \end{pmatrix}. \tag{A4}$$

Hence,

$$M_w = UDV^\dagger = (|u_0\rangle \quad |u_1\rangle)\begin{pmatrix} \sigma_+ & 0 \\ 0 & \sigma_- \end{pmatrix}\begin{pmatrix} \langle v_0| \\ \langle v_1| \end{pmatrix}. \tag{A5}$$

Here $\sigma_\pm$ are the *singular values* [by definition, they are the elements of the diagonal matrix D, Eq. (A3)]. If one writes $M_w = z_0\mathbf{I} + z_1\sigma_1 + z_2\sigma_2 + z_3\sigma_3$, where σ_i are Pauli matrices, then the expression for $\sigma_\pm$ turns out to be

$$\sigma_\pm = \sqrt{\sum_{i=0}^{3}|z_i|^2 \pm \sqrt{\left(\sum_{i=0}^{3}|z_i|^2\right)^2 - \left|z_0^2 - z_1^2 - z_2^2 - z_3^2\right|^2}}. \tag{A6}$$

Here, $z_0 = (a+d)/2$, $z_1 = (b+c)/2$, $z_2 = i(b-c)/2$, and $z_3 = (a-d)/2$, where a, b, c, and d are as defined in Eq. (A2). With this, the singular values are given by

$$\sigma_\pm = \sqrt{\frac{1}{2} \pm \sqrt{\frac{1}{4} - |ad - bd|^2}}. \tag{A7}$$

Here, use has been made of the normalization condition $|\langle w|w\rangle|^2 = |a|^2 + |b|^2 + |c|^2 + |d|^2 = 1$. Since $\sigma_+^2 + \sigma_-^2 = 1$, we redefine $\sigma_+ = \sqrt{\alpha}$ and $\sigma_- = \sqrt{1-\alpha}$. Therefore, from Eq. (A5), we have

$$M_w = \sqrt{\alpha}\,|u_0\rangle\langle v_0| + \sqrt{1-\alpha}\,|u_1\rangle\langle v_1| . \tag{A8}$$

Using this in Eq. (A1), we see that the tensor product state becomes

$$|w\rangle = \sqrt{\alpha}\,|u_0\rangle|v_0\rangle + \sqrt{1-\alpha}\,|u_1\rangle|v_1\rangle . \tag{A9}$$

Setting $|u_0\rangle = |0\rangle_u$, $|u_1\rangle = |1\rangle_u$, $|v_0\rangle = |1\rangle_v$, and $|v_1\rangle = |0\rangle_v$, we have

$$|w\rangle = \sqrt{\alpha}\,|01\rangle + \sqrt{1-\alpha}\,|10\rangle . \tag{A10}$$

This, however, should not be interpreted as the generation of an entangled state from a separable state. A separable state $|\psi\rangle = \frac{1}{2}(|00\rangle + |01\rangle + |10\rangle + |11\rangle)$, with $a = b = c = d = 1/2$, leads to $\alpha = 1$, and hence $|w\rangle = |01\rangle$.

[1] J. von Neumann, *Mathematical Foundations of Quantum Mechanics* (Princeton University Press, Princeton, 1995).
[2] C. M. Bender and S. Boettcher, Phys. Rev. Lett. **80**, 5243 (1998).
[3] Y. Xing, L. Qi, J. Cao, D.-Y. Wang, C.-H. Bai, H.-F. Wang, A.-D. Zhu, and S. Zhang, Phys. Rev. A **96**, 043810 (2017).
[4] T. Kato, *Perturbation Theory for Linear Operators* (Springer-Verlag, Berlin/Heidelberg, 1966).
[5] U. Günther, I. Rotter, and B. F. Samsonov, J. Phys. A: Math. Theor. **40**, 8815 (2007).
[6] A. Mostafazadeh, J. Math. Phys. **43**, 205 (2002).
[7] M. Müller and I. Rotter, Phys. Rev. A **80**, 042705 (2009).
[8] I. Rotter and J. Bird, Rep. Prog. Phys. **78**, 114001 (2015).
[9] A. Magunov, I. Rotter, and S. Strakhova, J. Phys. B **32**, 1489 (1999).
[10] A. Magunov, I. Rotter, and S. Strakhova, J. Phys. B **34**, 29 (2001).
[11] O. Atabek, R. Lefebvre, M. Lepers, A. Jaouadi, O. Dulieu, and V. Kokoouline, Phys. Rev. Lett. **106**, 173002 (2011).
[12] C. M. Bender, D. C. Brody, and H. F. Jones, Phys. Rev. D **70**, 025001 (2004).
[13] I. Rotter, J. Phys. A: Math. Theor. **42**, 153001 (2009).
[14] H. Eleuch and I. Rotter, Phys. Rev. A **95**, 022117 (2017).
[15] J. Heinrichs, Phys. Rev. B **63**, 165108 (2001).
[16] R. El-Ganainy, K. G. Makris, D. N. Christodoulides, and Z. H. Musslimani, Opt. Lett. **32**, 2632 (2007).
[17] K. G. Makris, R. El-Ganainy, D. N. Christodoulides, and Z. H. Musslimani, Phys. Rev. Lett. **100**, 103904 (2008).
[18] Z. H. Musslimani, K. G. Makris, R. El-Ganainy, and D. N. Christodoulides, Phys. Rev. Lett. **100**, 030402 (2008).
[19] X. Luo, J. Huang, H. Zhong, X. Qin, Q. Xie, Y. S. Kivshar, and C. Lee, Phys. Rev. Lett. **110**, 243902 (2013).
[20] C. Li, G. Zhang, X. Z. Zhang, and Z. Song, Phys. Rev. A **90**, 012103 (2014).
[21] G. L. Giorgi, Phys. Rev. B **82**, 052404 (2010).
[22] L. Zhang, G. S. Agarwal, W. P. Schleich, and M. O. Scully, Phys. Rev. A **96**, 013827 (2017).
[23] G. S. Agarwal and K. Qu, Phys. Rev. A **85**, 031802(R) (2012).
[24] L. Feng, Z. J. Wong, R.-M. Ma, Y. Wang, and X. Zhang, Science **346**, 972 (2014).
[25] H. Hodaei, M.-A. Miri, M. Heinrich, D. N. Christodoulides, and M. Khajavikhan, Science **346**, 975 (2014).

[26] L. Feng, Y.-L. Xu, W. S. Fegadolli, M.-H. Lu, J. E. Oliveira, V. R. Almeida, Y.-F. Chen, and A. Scherer, Nat. Mater. **12**, 108 (2013).

[27] J. Schindler, A. Li, M. C. Zheng, F. M. Ellis, and T. Kottos, Phys. Rev. A **84**, 040101(R) (2011).

[28] Y. D. Chong, L. Ge, H. Cao, and A. D. Stone, Phys. Rev. Lett. **105**, 053901 (2010).

[29] Z. Lin, H. Ramezani, T. Eichelkraut, T. Kottos, H. Cao, and D. N. Christodoulides, Phys. Rev. Lett. **106**, 213901 (2011).

[30] F. Nazari, M. Nazari, and M. K. Moravvej-Farshi, Opt. Lett. **36**, 4368 (2011).

[31] V. V. Konotop, J. Yang, and D. A. Zezyulin, Rev. Mod. Phys. **88**, 035002 (2016).

[32] S. Bittner, B. Dietz, U. Günther, H. L. Harney, M. Miski-Oglu, A. Richter, and F. Schäfer, Phys. Rev. Lett. **108**, 024101 (2012).

[33] S. Banerjee, *Open Quantum Systems: Dynamics of Nonclassical Evolution* (Springer, Berlin, 2018).

[34] H. Feshbach, Ann. Phys. **5**, 357 (1958).

[35] M. B. Plenio and P. L. Knight, Rev. Mod. Phys. **70**, 101 (1998).

[36] M. Jakob and S. Stenholm, Phys. Rev. A **70**, 012104 (2004).

[37] J. Naikoo, K. Thapliyal, S. Banerjee, and A. Pathak, Phys. Rev. A **99**, 023820 (2019).

[38] P. Malpani, N. Alam, K. Thapliyal, A. Pathak, V. Narayanan, and S. Banerjee, Ann. Phys. **531**, 1800318 (2019).

[39] K. Thapliyal, S. Banerjee, A. Pathak, S. Omkar, and V. Ravishankar, Ann. Phys. **362**, 261 (2015).

[40] J. Naikoo, K. Thapliyal, A. Pathak, and S. Banerjee, Phys. Rev. A **97**, 063840 (2018).

[41] H. S. Dhar, S. Banerjee, A. Chatterjee, and R. Ghosh, Ann. Phys. **331**, 97 (2013).

[42] S. Adhikari and S. Banerjee, Phys. Rev. A **86**, 062313 (2012).

[43] V. Sharma, C. Shukla, S. Banerjee, and A. Pathak, Quantum Inf. Proc. **14**, 3441 (2015).

[44] S. Luo, Phys. Rev. A **77**, 022301 (2008).

[45] I. Chakrabarty, S. Banerjee, and N. Siddharth, Quantum Inf. Comput. **11**, 0541 (2011).

[46] S. Banerjee, V. Ravishankar, and R. Srikanth, Ann. Phys. **325**, 816 (2010).

[47] S. Banerjee, V. Ravishankar, and R. Srikanth, Eur. Phys. J. D **56**, 277 (2010).

[48] A. Miranowicz, K. Bartkiewicz, A. Pathak, J. Peřina, Y.-N. Chen, and F. Nori, Phys. Rev. A **91**, 042309 (2015).

[49] A. Miranowicz, K. Bartkiewicz, N. Lambert, Y.-N. Chen, and F. Nori, Phys. Rev. A **92**, 062314 (2015).

[50] J. K. Asbóth, J. Calsamiglia, and H. Ritsch, Phys. Rev. Lett. **94**, 173602 (2005).

[51] K. Thapliyal, A. Pathak, B. Sen, and J. Peřina, Phys. Rev. A **90**, 013808 (2014).

[52] S. K. Giri, B. Sen, C. H. R. Ooi, and A. Pathak, Phys. Rev. A **89**, 033628 (2014).

[53] E. M. Graefe, U. Günther, H. Korsch, and A. Niederle, J. Phys. A: Math. Theor. **41**, 255206 (2008).

[54] S. Klaiman, U. Günther, and N. Moiseyev, Phys. Rev. Lett. **101**, 080402 (2008).

[55] I. Estermann and O. Stern, Z. Phys. **61**, 95 (1930).

[56] J. Lawall and M. Prentiss, Phys. Rev. Lett. **72**, 993 (1994).

[57] T. Pfau, C. Kurtsiefer, C. S. Adams, M. Sigel, and J. Mlynek, Phys. Rev. Lett. **71**, 3427 (1993).

[58] D. Cassettari, B. Hessmo, R. Folman, T. Maier, and J. Schmiedmayer, Phys. Rev. Lett. **85**, 5483 (2000).

[59] F. B. Dunning and R. G. Hulet, *Atomic, Molecular, and Optical Physics: Atoms and Molecules* (Academic Press, Cambridge, 1996).

[60] H. Fearn and R. Loudon, Opt. Commun. **64**, 485 (1987).

[61] M. A. Nielsen and I. Chuang, *Quantum Computation and Quantum Information* (Cambridge University Press, Cambridge, 2002).

[62] A. Barenco, C. H. Bennett, R. Cleve, D. P. DiVincenzo, N. Margolus, P. Shor, T. Sleator, J. A. Smolin, and H. Weinfurter, Phys. Rev. A **52**, 3457 (1995).

[63] B. R. Rao, R. Srikanth, C. M. Chandrashekar, and S. Banerjee, Phys. Rev. A **83**, 064302 (2011).

[64] C. H. Bennett, H. J. Bernstein, S. Popescu, and B. Schumacher, Phys. Rev. A **53**, 2046 (1996).

[65] S. Popescu and D. Rohrlich, Phys. Rev. A **56**, R3319 (1997).

[66] C. H. Bennett, D. P. DiVincenzo, J. A. Smolin, and W. K. Wootters, Phys. Rev. A **54**, 3824 (1996).

[67] V. Vedral, M. B. Plenio, M. A. Rippin, and P. L. Knight, Phys. Rev. Lett. **78**, 2275 (1997).

[68] V. Vedral and M. B. Plenio, Phys. Rev. A **57**, 1619 (1998).

[69] J. Eisert and M. B. Plenio, J. Mod. Opt. **46**, 145 (1999).

[70] K. Życzkowski, P. Horodecki, A. Sanpera, and M. Lewenstein, Phys. Rev. A **58**, 883 (1998).

[71] S. Hill and W. K. Wootters, Phys. Rev. Lett. **78**, 5022 (1997).

[72] A. K. Sarma and B. Prannay, arXiv:1408.6672.

[73] H.-j. Li, J.-p. Dou, and G. Huang, Opt. Express **21**, 32053 (2013).

[74] L. Du, Z. Xu, C. Yin, and L. Guo, Chin. Phys. Lett. **35**, 050301 (2018).

[75] J. Naikoo, S. Dutta, and S. Banerjee, Phys. Rev. A **99**, 042128 (2019).

[76] U. Shrikant, R. Srikanth, and S. Banerjee, Phys. Rev. A **98**, 032328 (2018).

[77] N. P. Kumar, S. Banerjee, and C. Chandrashekar, Sci. Rep. **8**, 8801 (2018).

[78] N. P. Kumar, S. Banerjee, R. Srikanth, V. Jagadish, and F. Petruccione, Open Syst. Info. Dynam. **25**, 1850014 (2018).

[79] G. Thomas, N. Siddharth, S. Banerjee, and S. Ghosh, Phys. Rev. E **97**, 062108 (2018).

[80] K. Thapliyal, A. Pathak, and S. Banerjee, Quantum Inf. Proc. **16**, 115 (2017).

[81] S. Banerjee, N. P. Kumar, R. Srikanth, V. Jagadish, and F. Petruccione, arXiv:1703.8004.

[82] S. Banerjee and R. Ghosh, J. Phys. A: Math. Theor. **40**, 13735 (2007).

[83] R. Srikanth and S. Banerjee, Phys. Rev. A **77**, 012318 (2008).

[84] S. Banerjee and R. Srikanth, Eur. Phys. J. D **46**, 335 (2008).

[85] A. De, A. Lang, D. Zhou, and R. Joynt, Phys. Rev. A **83**, 042331 (2011).

[86] R. L. Franco, A. D'Arrigo, G. Falci, G. Compagno, and E. Paladino, Phys. Scr. **2012**, 014019 (2012).

[87] S. K. Goyal, S. Banerjee, and S. Ghosh, Phys. Rev. A **85**, 012327 (2012).

[88] C. Benedetti, F. Buscemi, P. Bordone, and M. G. A. Paris, Phys. Rev. A **87**, 052328 (2013).

[89] S. Daffer, K. Wódkiewicz, J. D. Cresser, and J. K. McIver, Phys. Rev. A **70**, 010304(R) (2004).

[90] B. Horst, K. Bartkiewicz, and A. Miranowicz, Phys. Rev. A **87**, 042108 (2013).